http://dx.doi.org/10.5012/bkcs.2014.35.7.2004

Facile Synthesis of ZnO Nanoparticles and Their Photocatalytic Activity

Soo-Keun Lee,† A Young Kim,† Jun Young Lee, Sung Hyun Ko, and Sang Wook Kim*

*Department of Advanced Materials Chemistry, College of Science and Technology, Dongguk University-Gyeongju, Gyeongju, Gyeongbuk 780-714, Korea. *E-mail: swkim@dongguk.ac.kr*
†Nano & Bio Research Division, Daegu Gyeongbuk Institute of Science and Technology (DGIST), Daegu 711-873, Korea
Received January 20, 2014, Accepted March 10, 2014

This paper reports the facile synthesis methods of zinc oxide (ZnO) nanoparticles, **Z1**-**Z10**, using diethylene glycol (DEG) and polyethylene glycol (PEG400). The particle size and morphology were correlated with the PEG concentration and reaction time. With 0.75 mL of PEG400 in 150 mL of DEG and a 20 h reaction time, the ZnO nanoparticles began to disperse from a collective spherical grain shape. The ZnO nanoparticles were characterized by X-ray diffraction, scanning electron microscopy, transmission electron microscopy and a N_2 adsorption–desorption studies. The Brunauer-Emmett-Teller (BET) surface areas of **Z4**, **Z5** and **Z10** were 157.083, 141.559 and 233.249 m^2/g, respectively. The observed pore diameters of **Z4**, **Z5** and **Z10** were 63.4, 42.0 and 134.0 Å, respectively. The pore volumes of **Z4**, **Z5** and **Z10** were 0.249, 0.148 and 0.781 cm^3/g, respectively. The photocatalytic activity of the synthesized ZnO nanoparticles was evaluated by methylene blue (MB) degradation, and the activity showed a good correlation with the N_2 adsorption–desorption data.

Key Words : Zinc oxide, Photocatalytic activity, Methylene blue degradation, Nanosphere, Nanoparticle synthesis

Introduction

Zinc oxide (ZnO) nanoparticles has attracted considerable interest because of their promising applications in a range of fields, such as solar cell research,[1,2] photocatalysts,[3] transparent conducting thin films for semiconductors,[4] electrical devices for light emitting diodes,[4] bioimaging, and biomedical applications.[5-7] Obtaining monodisperse nanoparticles and controlling the particle size and shape are important factors for utilizing ZnO.

The key factors affecting the agglomeration of the synthesized nanoparticles are the large surface area and surface energy. Therefore, a variety of synthesis methods for ZnO nanoparticles to prevent agglomeration have been reported.[8-11] Polyol-mediated synthesis method is a well-known method for synthesizing metal oxide nanoparticles including ZnO.[8-11]

Polyols act as both a solvent and stabilizing agent that prevent particle agglomeration.[12] Jezequel first reported the synthesis of monodisperse ZnO sphere nanoparticles using diethylene glycol (DEG).[13] Chieng *et al.* developed the modified polyol methods to obtain monodisperse ZnO nanoparticles with a controllable size and shape by varying the glycol length.[14] Abraham *et al.* reported the spherical ZnO nanoparticles consisting of colloidal sub-unit (cauliflower like nanoparticles) using an autoclave method and DEG as a solvent.[11] Zhai *et al.* reported the synthesis of core/shell structured ZnO/SiO_2 nanoparticles using a mixture of DEG and PEG and their photocatalytic activity using Rhodamine B degradation as a test compound. The synthesized ZnO nanoparticles were 15-20 nm in diameter.[15]

The purpose of this study is to synthesize ZnO nanoparticles having promising photocatalytic activities. Hence, cauliflower-like nanospheres of ~200 nm consisting of few nanometer ZnO nanoparticles in diameter have been prepared as a target ZnO due to its high surface area, which can be useful for photocatalysis. Among the diverse ZnO nanoparticles synthesis methods, DEG-mediated hydrothermal synthesis protocol has been applied except NaOH addition because it has been known that the mean particle size can be tailored by adjusting the reaction temperature to 180-240 °C and time to 2-12 h.[12] While DEG acts as a stabilizer and limiting agent for particle growth, PEG400 can help the growth of ZnO nuclei.[16-20] This paper describes DEG and PEG400-mediated ZnO synthesis results in detail. The ZnO nanoparticles were characterized by X-ray diffraction (XRD), scanning electron microscopy (SEM), transmission electron microscopy (TEM) and a N_2 adsorption–desorption studies. The photocatalytic degradation of methylene blue (MB) using the prepared ZnO nanoparticles was also examined.

Experimental

Reagents, Standards and Samples. Zinc (II) acetate dihydrate ($Zn(CH_3COO)_2 \cdot 2H_2O$) was purchased from Sigma-Aldrich. Diethylene glycol (DEG, Junsei) and polyethylene glycol (PEG, MW 400, Samchun) were used as the solvents. All other reagents were of analytical grade and used as received.

Characterization and Measurements. The ZnO nanoparticles were characterized by scanning electron microscopy (SEM, Hitachi, S-4800), transmission electron microscopy (TEM, Hitachi, HF-3300). The crystallinity of the ZnO nanoparticles was characterized by X-ray diffraction (XRD, Bruker, D2 PHASER). The surface area, pore size and BJH

Table 1. Reaction conditions for ZnO nanoparticles synthesis

Sample number	Zinc acetate (g)	DEG (mL)	PEG (mL)	Reaction time (h)	Mean Particle size (nm)	Zinc acetate Conc. (g/mL)	PEG/DEG (V/V)
Z1	2	150	0.25	12	100-200	0.013	0.002
Z2	2.2	150	0.25	12	100-200	0.015	0.002
Z3	2.4	150	0.25	12	100-200	0.016	0.002
Z4	2	150	0.15	12	100-200	0.013	0.001
Z5	2	150	0.35	12	100-300	0.013	0.002
Z6	2	100	0.25	12	100-300	0.020	0.003
Z7	2	200	0.25	12	50-150	0.010	0.001
Z8	2	150	0.25	20	50-150	0.012	0.002
Z9	2	150	0.5	20	50-150	0.012	0.002
Z10	2	150	0.75	20	Less than 100 and scattered	0.012	0.005

pore diameter were examined using a N_2 adsorption–desorption study (Micromeritics ASAP-2010, USA).

Synthesis of ZnO Nanoparticles. Zinc (II) acetate dihydrate (2.0-2.4 g) was added to DEG (150 mL) in a 3 neck flask. The flask was exposed to ultrasound to disperse the reaction mixture. Subsequently, 0.15-0.75 mL of PEG, which was well dispersed in absolute ethanol, was added to the reaction mixture. The reaction mixtures were allowed to react at 180 °C for either 12 h or 20 h. The precipitates were washed 3 times with ethanol for and centrifuged (4,000 rpm, 15 min) to give the ZnO nanoparticles. The nanoparticles were dried under vacuum 12 h. Sample numbers of **Z1** to **Z10** as well as the synthesis conditions are tabulated in Table 1.

Photocatalytic Activity Measurements of the ZnO Nanoparticles. Zinc oxide nanoparticles can be utilized in the photochemical and electrical materials industry. Therefore, the photocatalytic activities of selected nanoparticles (**Z4**, **Z5**, **Z10**) have been measured on the MB degradation test. The decomposition of MB was monitored using a UV-visible spectrophotometer (Varian Cary 50). ZnO nanoparticles were dispersed in a 0.01 mM methylene blue solution (0.5 g/L) and irradiated with six UVB lamps (8 W, λ_{max} at 365 nm) to compare the photocatalytic activity.

Results and Discussion

Characterization. The prepared ZnO nanoparticles were characterized by N_2 adsorption–desorption isotherm, SEM, TEM, TGA, XRD. Table 2 lists the Brunauer-Emmett-Teller (BET) surface area,[21] Barret–Joyner–Halenda (BJH) pore diameter, and total pore volumes.

X-ray Diffraction. Figure 1 shows the XRD patterns of the prepared ZnO nanoparticles (**Z4**, **Z5** and **Z10**). The XRD patterns of the ZnO nanoparticles were in agreement with reported data,[3-7] suggesting that all samples were the hexagonal phase (JCPDS 01-075-0576 wurtzite structure). No peaks for other phases were observed. These results showed that the shape of the ZnO nanoparticles did not affect the ZnO crystal structure regardless of whether the nanoparticles were dispersed or gathered like a cauliflower. The mean crystal sizes of **Z4**, **Z5** and **Z10** were calculated based on the Scherrer equation $D = 0.9\lambda/B\cos\theta$, where D, λ, B, and θ, are the mean grain size, wavelength of X-ray (0.154 nm), full width at half maximum (FWHM) of the (100) and (101) peaks, and the Bragg diffraction angle, respectively. The calculated mean grain size of **Z4**, **Z5** and **Z10** were 5.25 nm, 3.5 nm and 4.2 nm, respectively.

Table 2. BET surface area, total pore volume and BJH pore diameter of **Z4**, **Z5** and **Z10**

Sample	BET Surface Area (m^2/g)	Total Pore Volume (cm^3/g)	BJH Pore Diameter (Å)
Z4	157.083	0.249	63.4
Z5	141.559	0.148	42.0
Z10	233.249	0.781	134.0

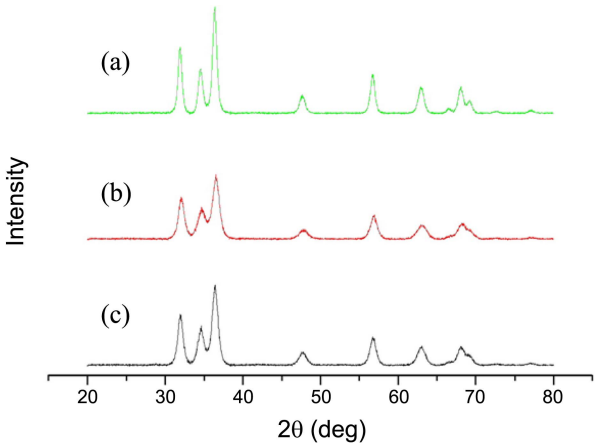

Figure 1. XRD patterns of **Z4**, **Z5**, and **Z10**.

Characterization by SEM and TEM. SEM images of **Z5** and **Z10** showed clear differences (Fig. 2). The shape of **Z5** was nanospheres consisting of small grains, 3-5 nm in diameter. In contrast, **Z10** consisted of both nanospheres (but total collective size was small compared to **Z5**) and dispersed nanoparticles, suggesting that the nanoparticles

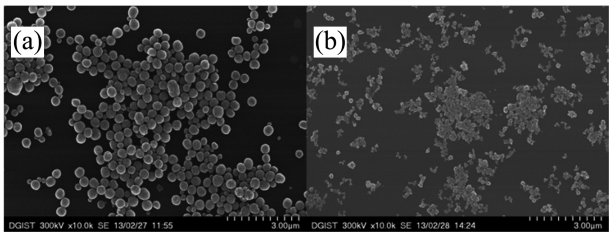

Figure 2. SEM images of (a) **Z5** and (b) **Z10**.

began to disperse in a mixed shape. These reaction conditions were reconfirmed with additional reactions. Figure 3 presents TEM images of all other samples, which supports these results. As shown in Figure 3, all samples except **Z10** showed well-ordered spherical type nanospheres, even though the particle porosity varied significantly. These cauliflower like nanospheres were fabricated by the aggregation of small particles, which presumably led to a rough surface and large particle porosity.[5,7-9]

The mean particle sizes of ZnO produced were slightly dependant on zinc acetate concentration and no dependency was observed in reaction time.

ZnO nanoparticles shape was possibly influenced by PEG/DEG (V/V) concentration. While the driving force by DEG as a chelating agent dominates the ZnO nanospheres formation at low PEG/DEG (V/V) concentration ratio of 0.001-0.003, scattering phenomenon was observed at ratio of 0.005 (Table 1).

This can be attributed to the results of two conflict effects from DEG and PEG. DEG can be act as a chelating agent, so the ZnO nanoparticles are chelated to the DEG, which generates stable and relatively tightly bounded nanospheres to a certain extent (30-200 nm).[12] Li *et al.* reported that when ZnO nanoparticles are synthesized in the presence of PEG400 without DEG, PEG400 concentration of 12.5%-25.0% can produce column shape ZnO nanoparticles and 50.0% PEG can produce spherical shape ZnO nanoparticles with ~46 nm in diameters with loose sphere density.[16] Thus, ZnO nanoparticles nucleation by DEG is more effective at the low concentration range of PEG, but as PEG concentration

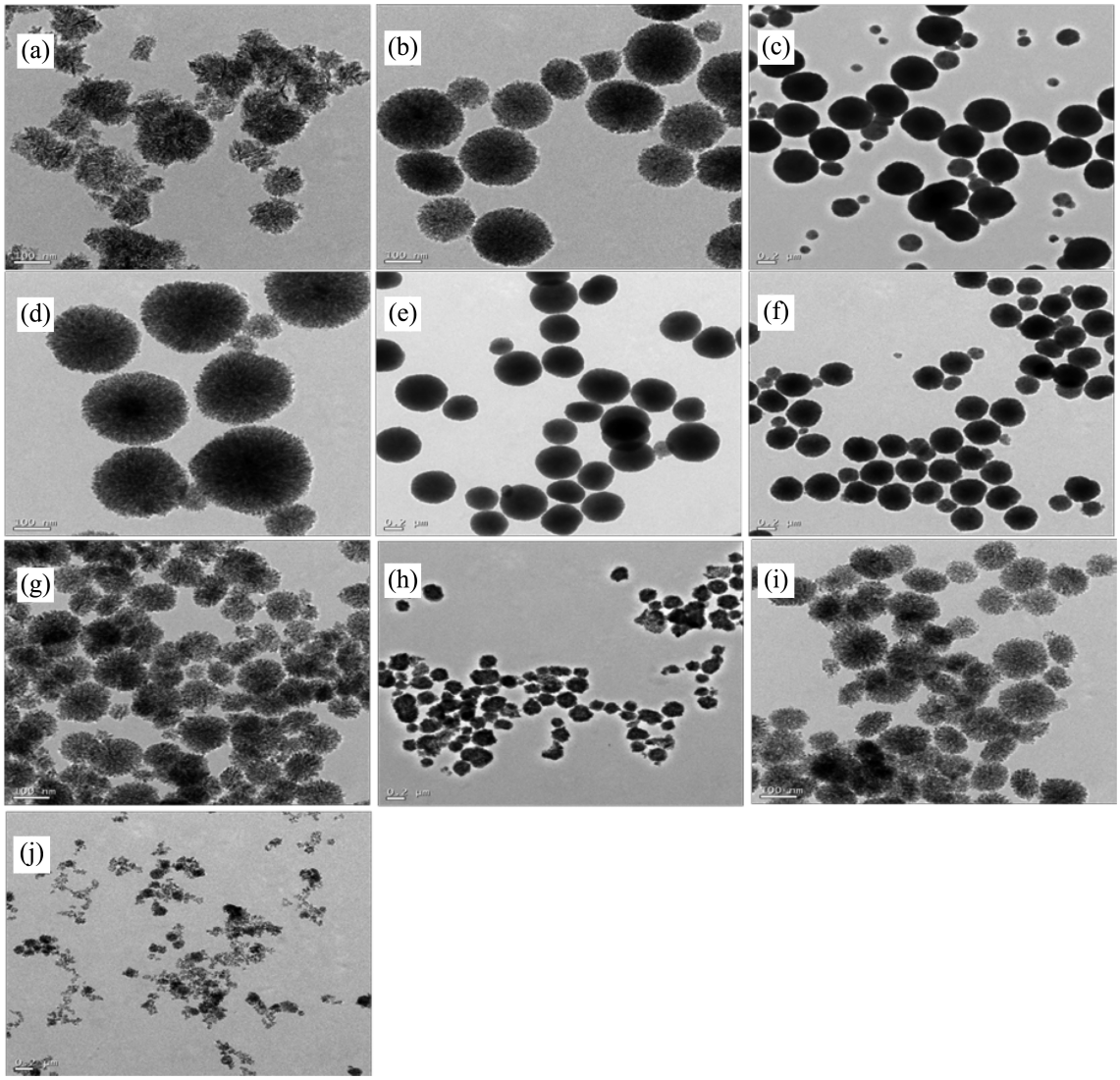

Figure 3. TEM images of (a) **Z1**, (b) **Z2**, (c) **Z3**, (d) **Z4**, (e) **Z5**, (f) **Z6**, (g) **Z7**, (h) **Z8**, (i) **Z9** and (j) **Z10**.

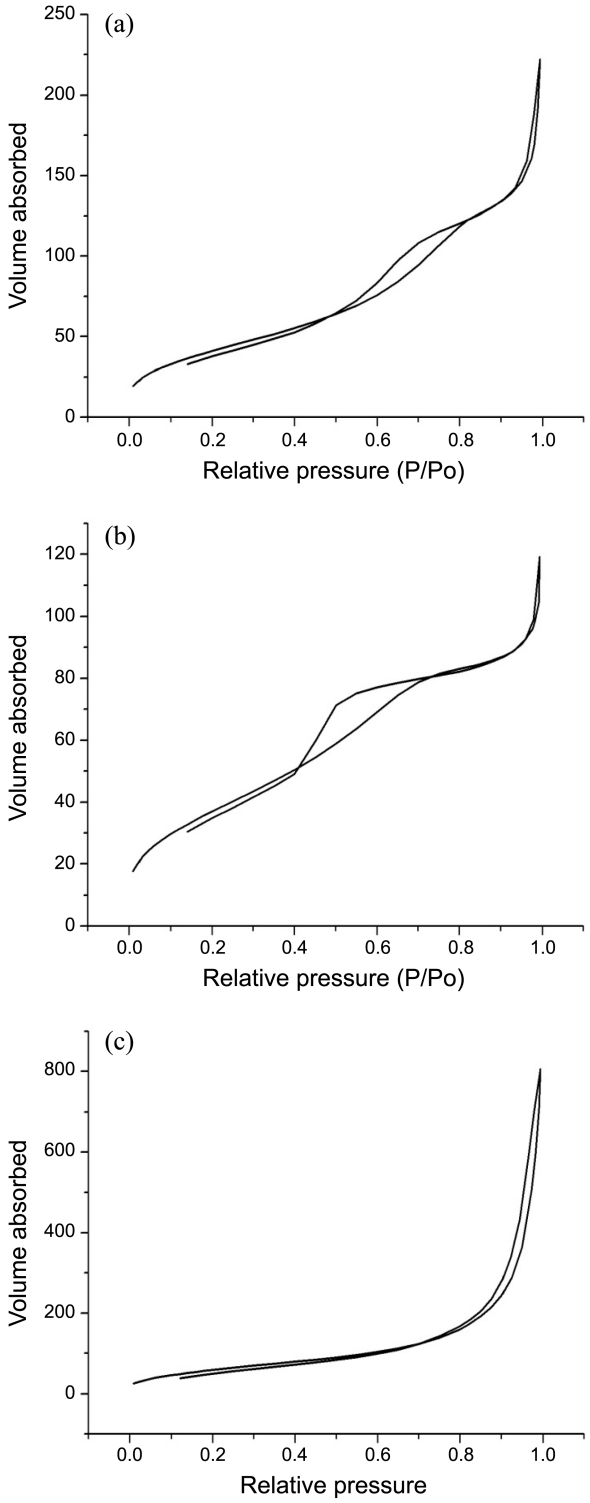

Figure 4. N_2 adsorption/desorption isotherms of (a) **Z4**, (b) **Z5** and (c) **Z10**.

increase, particles in the sphere get loosen and more scattered.

Nitrogen Adsorption-Desorption Study. The total pore volume of the material was estimated from the level of N_2 adsorption at a relative pressure of approximately 0.995. The primary mesopore volume V_p was calculated from the slope of the linear portion of the t-plot in the pressure range above

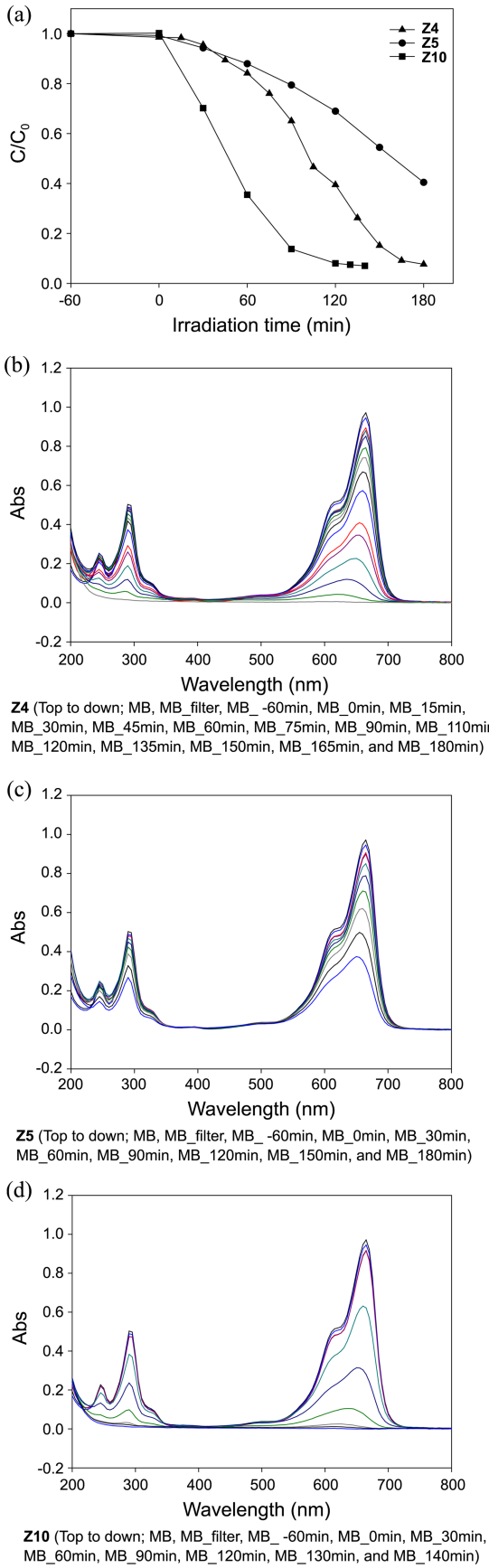

Z4 (Top to down; MB, MB_filter, MB_ -60min, MB_0min, MB_15min, MB_30min, MB_45min, MB_60min, MB_75min, MB_90min, MB_110min, MB_120min, MB_135min, MB_150min, MB_165min, and MB_180min)

Z5 (Top to down; MB, MB_filter, MB_ -60min, MB_0min, MB_30min, MB_60min, MB_90min, MB_120min, MB_150min, and MB_180min)

Z10 (Top to down; MB, MB_filter, MB_ -60min, MB_0min, MB_30min, MB_60min, MB_90min, MB_120min, MB_130min, and MB_140min)

Figure 5. UV/Vis spectra of methylene blue (MB) depending on the UVB irradiation time (a) comparison graph of the three samples, (b) UV/Vis spectra of MB with **Z4**, (c) **Z5** and (d) **Z10**.

the pressure of nitrogen condensation in the primary pores. Figure 4 presents typical isotherms of the three ZnO nanoparticles. For the **Z4** sample, the isotherm revealed two characteristics, which were type II (IUPAC classification; mixed micro- and meso-porosity generate this isotherm) with some contribution of the type IV pore structure in the relative pressure range, 0.55-1.0.[22] Two hysteresis loops can be found in the same range, suggesting that there are two pore size distributions in different regions. The small hysteresis in the higher relative pressure range of 0.95-1.0 can be classified as a type H3 loop, which can be attributed to slit-shaped pores or plate-like particles.[23] The **Z5** sample showed similar characteristics to **Z4** except that the first hysteresis was observed in the pressure range of 0.4-0.7. In case of the **Z10** sample, the isotherm showed a slightly larger pore size and broader size distribution compared to **Z4** or **Z5**, which can be classified as the type H3 loop. Table 2 lists the BET surface area, BJH pore diameter, and total pore volume. The BET surface area of **Z4**, **Z5** and **Z10** was 157.083 m^2/g, 141.559 m^2/g and 233.249 m^2/g, respectively. The observed pore diameter for **Z4**, **Z5** and **Z10** were 63.4, 42.0 and 134.0 Å, respectively. The pore volumes of **Z4**, **Z5** and **Z10** were 0.249, 0.148 and 0.781 cm^3/g, respectively.[5,7]

Degradation Study of ZnO Nanoparticles using Methylene Blue. Methylene blue (MB) decomposition using the three catalysts was also investigated. MB is potentially harmful to the environment so its degradation has attracted considerable attention. Figure 5 shows UV/Vis spectral changes of MB depending on the UVB irradiation time. The spectrum of MB exhibits a major absorbance at 664 nm. The absorbance peak became weaker in intensity with time and totally disappeared after 150 min for **Z10** (120 min) and **Z4** (150 min), whereas the decomposition of MB by **Z5** was less effective. The reason for the low effectiveness is still under investigation but both **Z4** and **Z5** showed a similar structure, shape, pore and surface structure. Nevertheless, the effective degradation of MB with **Z10** can be attributed to its higher BET surface area, total pore volume and diameter.[3,10-12]

Conclusions

ZnO nanoparticles, ranging from nanospherical to a dispersed form in shape, were synthesized using DEG and PEG and morphology of particles was found to be controlled by varying the PEG concentration and reaction time. The mean grain sizes were determined by XRD and morphology and shape of particles were well characterized by SEM as well as TEM. The particle chararateristics such as porosity, surface areas, pore volumes and photocatalytic activity were determined by N_2 adsorption–desorption and degradation of MB. The key factors affecting particle morphology were PEG concentration and reaction time. Photocatalytic activity of ZnO nanoparticles was directly correlated with BET surface area, total pore volume and BJH pore diameter. Overall, these ZnO nanoparticles catalysts are expected to find applications in photochemical devices using ZnO in dye-sensitized solar cells.

Acknowledgments. This study was supported by the National Research Foundation of Korea (NRF- 2013M2A2A7059045) and the basic research program (14-NB-03) of the DGIST grant funded by the Korea Government (MSIP) and Dongguk University–Gyeongju Research Fund.

Referencess

1. Oh, H.; Krantz, J.; Litzov, I.; Stubhan, T.; Pinna, L.; Brabec, C. *Sol. Energ. Mat. & Sol. C* **2011**, *95*. 2194.
2. Song, D.; Aberle, A. G.; Xia, J. *Appl. Surf. Sci.* **2002**, *195*, 291.
3. Samah, M.; Merabet, S.; Bouguerra, M.; Ouhenia, S.; Bouzaza, A. *Kinet. Catal.* **2011**, *52*, 34.
4. Tsay, C.-Y.; Wu, C.-W.; Lei, C.-M.; Chen, F.-S.; Lin, C.-K. *Thin Solid Films* **2010**, *519*, 1516.
5. Tachikawa, S.; Noguchi, A.; Tsuge, T.; Hara, M.; Odawara, O.; Wada, H. *Materials* **2011**, *4*(6), 1132.
6. Bharda, P.; Mitra, M. K.; Das, G. C.; Dey, R.; Mukherjee, S. *Int. J. Environ. Sci. Te.* **2012**, *4*, 4223.
7. Ansari, S. A.; Husain, Q.; Qayum, S.; Azam, A. *Food. Chem. Toxicol.* **2011**, *49*, 2107.
8. Hong, R.; Pan, T.; Qian, J.; Li, H. Z. *Chem. Eng. J.* **2006**, *119*, 71.
9. Zhang, Y.; Chung, J. Y.; Lee, J. Y.; Myoung, J. H.; Lim, S. W. *J. Phys. Chem. Solids* **2011**, *72*, 1548.
10. Han, K.; Zhao, Z.; Xiang, Z.; Wang, C.; Zhang, J.; Yang, B. *Mater. Lett.* **2007**, *61*, 363.
11. Abraham, N.; Sebok, D.; Papp, Sz.; Korosi, L.; Dekany, I. *Colloid. Surface A* **2011**, *384*, 80.
12. Feldmann, C. *Adv. Funct. Mater.* **2003**, *13*, 101.
13. Jezequel, D.; Guenot, J.; Jouini, N.; Fievet, F. *J. Mater. Res.* **1995**, *10*, 77.
14. Chieng, B. W.; Loo, Y. Y. *Mater. Lett.* **2012**, *73*, 78.
15. Zhai, J.; Tao, X.; Pu, Y.; Zeng, X.-F.; Chen, J.-F. *Appl. Surf. Sci.* **2010**, *257*, 393.
16. Li, X.; He, G.; Xiao, G.; Liu, H.; Wang, M. *J. Colloid. Interf. Sci.* **2009**, *333*, 465.
17. Li, Z.; Xiong, Y.; Xie, Yi. *Inorg. Chem.* **2003**, *42*, 8105.
18. Liu, J.; Huang, X.; Li, Y.; Sulieman, K. M.; Sun, F.; He, X. *Scripta Mater.* **2006**, *55*, 795.
19. Hou, X.; Zhou, F.; Liu, W. *Mater. Lett.* **2006**, *60*, 3786.
20. Wang, W.; Zhan, Y.; Wang, G. *Chem. Comm.* **2001**, 727.
21. Brunauer, S.; Emmett, P. H.; Teller, E. *J. Am. Chem. Soc.* **1938**, *60*, 309.
22. Kruk, M.; Jaroniec, M. *Chem. Mater.* **2001**, *13*, 3169.
23. Yu, J. G.; Liu, W.; Yu, H. G. *Cryst. Growth. Des.* **2008**, *8*, 930.